THE JOURNAL OF BIOLOGICAL CHEMISTRY
Vol. 276, No. 45, Issue of November 9, pp. 42311–42321, 2001
Printed in U.S.A.

6-*O*-Sulfotransferase-1 Represents a Critical Enzyme in the Anticoagulant Heparan Sulfate Biosynthetic Pathway*

Received for publication, February 14, 2001, and in revised form, September 6, 2001
Published, JBC Papers in Press, September 10, 2001, DOI 10.1074/jbc.M101441200

Lijuan Zhang‡§¶, David L. Beeler‡, Roger Lawrence‡, Miroslaw Lech‡, Jian Liu‖, Joseph C. Davis, Zachary Shriver**, Ram Sasisekharan**, and Robert D. Rosenberg‡¶‡‡**

*From the ‡Department of Biology, **Division of Bioengineering, Environmental Health Medicine, Massachusetts Institute of Technology, Cambridge, Massachusetts 02139, and ¶Department of Medicine, Harvard Medical School, BIDMC, Boston, Massachusetts 02215*

Using recombinant retroviral transduction, we have introduced the heparin/heparan sulfate (HS) 3-*O*-sulfotransferase 1 (*3-OST-1*) gene into Chinese hamster ovary (CHO) cells. Expression of *3-OST-1* confers upon CHO cells the ability to produce anticoagulantly active HS (HS^{act}). To understand how *6-OST* and other proteins regulate HS^{act} biosynthesis, a CHO cell clone with three copies of *3-OST-1* was chemically mutagenized. Resulting mutants that make HS but are defective in generating HS^{act} were single-cell-cloned. One cell mutant makes fewer 6-*O*-sulfated residues. Modification of HS chains from the mutant with pure *6-OST-1* and 3′-phosphoadenosine 5′-phosphosulfate increased HS^{act} from 7% to 51%. Transfection of this mutant with *6-OST-1* created a CHO cell line that makes HS, 50% of which is HS^{act}. We discovered in this study that (i) *6-OST-1* is a limiting enzyme in the HS^{act} biosynthetic pathway *in vivo* when the limiting nature of *3-OST-1* is removed; (ii) HS chains from the mutant cells serve as an excellent substrate for demonstrating that *6-OST-1* is the limiting factor for HS^{act} generation *in vitro*; (iii) in contradiction to the literature, *6-OST-1* can add 6-*O*-sulfate to GlcNAc residues, especially the critical 6-*O*-sulfate in the antithrombin binding motif; (iv) both 3-*O*- and 6-*O*-sulfation can be the final step in HS^{act} biosynthesis in contrast to prior publications that concluded 3-*O*-sulfation is the final step in HS^{act} biosynthesis; (v), in the presence of HS interacting protein peptide, 3-*O*-sulfate-containing sugars can be degraded into disaccharides by heparitinase digestion as demonstrated by capillary high performance liquid chromatography coupled with mass spectrometry.

Heparin/heparan sulfate (HS)[1] is a linear polymer covalently attached to the protein cores of proteoglycans, which are abundant and ubiquitously expressed in almost all animal cells. HS is assembled by the action of a large family of enzymes that catalyze chain polymerization (alternating addition of GlcNAc and GlcUA residues), GlcNAc *N*-deacetylation and *N*-sulfation, glucuronic acid (GlcUA) epimerization to L-iduronic acid (IdoUA), 2-*O*-sulfation of uronic acid residues, and 3-*O*- and 6-*O*-sulfation of glucosaminyl residues. Tissue-specific and developmentally regulated expression of the biosynthetic enzymes and enzyme isoforms produces HS chains with distinct sequences (1–3). These different sequences enable interactions to occur with a broad array of protein ligands that modulate a wide range of biological functions in development, differentiation, homeostasis, and bacterial/viral entry (reviewed in Refs. 4–11).

The specificity of any HS and protein interaction is largely dictated by arrangements of sulfates along the chain. For example, the pentasaccharide sequence, GlcNAc/NS**6S**-GlcUA-GlcNS**3S±**6S-IdoUA2S-GlcNS6S, represents the minimum sequence for antithrombin (AT) binding, where the **3S** (3-*O*-sulfate) and **6S** (6-*O*-sulfate) groups constitute the most critical elements involved in the interaction (12–16). To delineate the biosynthetic pathway that regulates anticoagulant heparan sulfate (HS^{act}) biosynthesis, our laboratory has purified as well as molecularly cloned *3-OST-1* (17,18). We have demonstrated that *3-OST-1*, usually existing in limited amounts, acts upon HS^{act} precursor to produce HS^{act} and upon HS^{inact} precursor to produce 3-*O*-sulfated HS^{inact} (17, 19). When *3-OST-1* is no longer limiting, the capacity for HS^{act} generation is determined by the abundance of HS^{act} precursors (20). In this case, the limitation in HS^{act} production is the presence of the critical 6-*O*-sulfate groups and/or the availability of proper epimerization/sulfation patterns in the precursors.

In most cases, the critical 6S in the AT binding oligosaccharides sequenced and characterized in heparin is attached to GlcNAc residues (a summary table for heparin is presented in Refs. 21, 22). We previously reported that the critical 6S in

* This work was supported in part by National Institutes of Health Grants 5-P01-HL41484 and 5-R01-HL58479 (to R. D. R.) and GM-50573 (to R. S.). The costs of publication of this article were defrayed in part by the payment of page charges. This article must therefore be hereby marked "*advertisement*" in accordance with 18 U.S.C. Section 1734 solely to indicate this fact.

The nucleotide sequence(s) reported in this paper has been submitted to the GenBank™/EBI Data Bank with accession number(s) AB006180.

§ Recipient of National Research Service Award Postdoctoral Fellowship.

‖ Current address: Division of Medicinal Chemistry, School of Pharmacy, University of North Carolina, Chapel Hill, NC 27599.

‡‡ To whom correspondence should be addressed: Massachusetts Institute of Technology, Bldg. 68-480, 77 Massachusetts Ave., Cambridge, MA 02139. Tel.: 617-253-8804; Fax: 617-258-6553; E-mail: rdrrosen@mit.edu.

[1] The abbreviations used are: HS, heparan sulfate; HS^{act}, anticoagulantly active heparan sulfate; HS^{inact}, anticoagulantly inactive heparan sulfate; HS^{total}, total heparan sulfate; CHAPS, 3-[(3-cholamidopropy)dimethylammonio]-1-propanesulfonic acid; GAG, glycosaminoglycan; PAPS, 3′-phosphoadenosine 5′-phosphosulfate; AT, antithrombin; *3-OST-1*, glucosaminyl 3-*O*-sulfotransferase-1; *6-OST-1*, *-2*, *-3*, glucosaminyl 6-*O*-sulfotransferase-1, -2, -3; GlcUA, glucuronic acid; IdoUA, iduronic acid; 2S, 2-*O*-sulfate; 3S, 3-*O*-sulfate; 6S, 6-*O*-sulfate; NS, *N*-sulfate; PBS, phosphate-buffered saline; CHO, Chinese hamster ovary; HIP, heparin/heparan sulfate interacting protein; IPRP-HPLC, ion pairing reverse phase-high pressure liquid chromatography; ESI-MS, electrospray ionization-mass spectrometry; FGF, fibroblast growth factor; FGFR, FGF receptor; RT-PCR, reverse transcriptase-polymerase chain reaction; MES, 4-morpholineethanesulfonic acid; bp, base pair(s); UTR, untranslated repeat; nt, nucleotide(s); CDSNS-heparin, *N*-, *O*-desulfated, re-*N*-sulfated heparin.

HS^{act} from F9 cells is exclusively attached to GlcNAc residues (20). To date, three 6-*O*-sulfotransferases have been cloned, but reported substrate specificities indicate that none of them can put a 6-*O*-sulfate group on GlcNAc residues (2). To understand how specific 6-*O*-sulfotransferases and other factors regulate HS^{act} biosynthesis, we created cell mutants that are defective in the formation of HS^{act} precursors. We chose Chinese hamster ovary (CHO) cells, because a series of HS biosynthetic mutants have been successfully made in this cell line (23–28). However, CHO wild-type cells do not generate 3-*O*-sulfated residues and therefore do not make any HS^{act}. Using recombinant retroviral transduction, we have introduced the HS 3-*O*-sulfotransferase-1 (*3-OST-1*) gene into CHO cells (29). 3-OST-1 expression gives rise to CHO cells with the ability to produce HS^{act}. A cell line was chosen that has three copies of *3-OST-1* as determined by Southern analysis (29). After chemical mutagenesis of this cell line, mutant cells that were positive for FGF-2 binding but negative for AT binding were FACS sorted and cloned. The scheme for making HS^{act} precursor mutants is outlined in Fig. 1. The advantage of having multiple copies of 3-OST-1 is that other upstream genes that are responsible for generating specific HS precursor structures can be sought after chemical mutagenesis without concern for the loss of *3-OST-1*. FGF-2 selection is employed to ensure that the mutant cells still make HS. By using this scheme, we obtained a 6-*O*-sulfate-defective mutant. After correcting the mutant with 6-*O*-sulfotransferase-1 transfection, we created a cell line that makes HS, 50% of which is HS^{act}. This represents the highest percentage of HS^{act} production by any cell line reported so far.

The approach used in this study includes placing multiple copies of a downstream enzyme in CHO cells, mutagenizing the cells to obtain mutants deficient in upstream enzymes that are part of the pathway, and then characterizing the mutants. This technique may constitute a general approach for defining and obtaining the components of biosynthetic pathways once the terminal biosynthetic enzyme has been obtained and proteins that recognize the final product of the pathway are available.

EXPERIMENTAL PROCEDURES

Cell Culture—Wild-type Chinese hamster ovary cells (CHO-K1) were obtained from the American Type Culture Collection (CCL-61, ATCC, Rockville, MD). Wild-type and mutant cells were maintained in Ham's F-12 medium supplemented with 10% fetal bovine serum (HyClone), penicillin G (100 units/ml), and streptomycin sulfate (100 μg/ml) at 37 °C under an atmosphere of 5% CO_2 in air and 100% relative humidity. The cells were passaged every 3–4 days with 0.125% (w/v) trypsin and 1 mM EDTA, and after 10–15 cycles, fresh cells were revived from stocks stored under liquid nitrogen. Low-sulfate medium was composed of Ham's F-12 medium supplemented with penicillin G (100 units/ml) and 10% fetal bovine serum that had been dialyzed 200-fold against phosphate-buffered saline (PBS) (30). Low-glucose Ham's F-12 medium contained 1 mM glucose supplemented with penicillin G (100 units/ml), streptomycin sulfate (100 μg/ml), and fetal bovine serum that had been dialyzed 200-fold against PBS (30). All tissue culture media and reagents were purchased from Life Technologies, Inc. (Gaithersburg, MD) unless otherwise indicated.

3-OST-1 Recombinant Retroviral Transduction—The method of 3-OST-1 recombinant retroviral transduction into CHO cells was described in detail in our previous publication (29).

Antithrombin and FGF-2 Labeling—The same procedure has been used as described previously (29).

Cell Sorting—Nearly confluent monolayers of *3-OST-1*-transduced CHO-K1 cells were detached by adding 10 ml of 2 mM EDTA in PBS containing 10% fetal bovine serum and centrifuged. The cell pellets were placed on ice, and 50 μl each of fluorescein-AT and Alexa 594-FGF-2 were added. After 30 min, the cells were washed once and resuspended in 1 ml of 10% fetal bovine serum in PBS containing 2 mM EDTA. Flow cytometry and cell sorting was performed on FACScan and FACStar instruments (Becton Dickinson) using dual color detection filters. Cells positive for AT and FGF-2 binding were sorted and subsequently single-cell-cloned into a 96-well plate. The single-cell clones were expanded and frozen for further analysis.

Twelve *3-OST-1*-transduced CHO-K1 clones were obtained as described above. The number of copies of *3-OST-1* in the individual clones was determined by Southern analysis. Genomic DNA (10 μg) was digested with 40 units of *Eco*RI overnight at 37 °C, electrophoresed on a 0.7% (w/v) agarose gel, transferred to GeneScreen Plus (PerkinElmer Life Sciences), and probed with 3-OST-1 cDNA labeled with the Megaprime labeling kit (Amersham Pharmacia Biotech). Blots were hybridized in ExpressHyb solution (CLONTECH) containing *3-OST-1* probe (2×10^6 cpm/ml), followed by autoradiography. The cell clone with three copies of *3-OST-1* was expanded and frozen for further studies.

Mutant Screening—Wild-type CHO cells with three copies of *3-OST-1* were mutagenized with ethylmethane sulfonate as described in the literature (31) and frozen under liquid nitrogen. A portion of cells was thawed, propagated for 3 days, and labeled with both Alexa 594-FGF-2 and fluorescein-AT. The labeled cells were sorted, and FGF-2-positive and AT-negative cells were collected. Approximately 1×10^4 sorted cells were collected into 1 ml of complete F-12 Ham's media then plated in T-75 flasks. Sorted cell populations were maintained in complete F-12 Ham's medium for 1 week, then the cells were labeled and sorted again as described above. After five rounds of sorting, FGF-2-positive and AT-negative cells were single-cell-sorted into a 96-well plate. The single-cell clones were expanded and frozen for further analysis. The sorting profiles of CHO-K1 with three copies of *3-OST-1*, mutant, and the *6-OST-1* correctant of the mutant were shown by dual-color fluorescence flow cytometric analysis (see Fig. 2)

HS Preparation and Analysis—The method was the same as one published previously (29).

cDNA Cloning and Expression of CHO 6-OST-1—Sequences coding for CHO *6-OST-1* were amplified from a CHO-K1/cDNA quick-clone library (CLONTECH). The reaction mixture contained 2 units of *Pfu* polymerase (Stratagene), 1 ng of cDNA, and 100 pmol of the primers. The sense primer has an added *Bgl*II site (5′-GCAGATCTGCAGGAC-CATGGTTGAGCGCGCCAGCAAGTTC-3′), and the antisense primer has an added *Xba*I site (5′-GCTCTAGACTACCACTTCTCAATGATGT-GGCTC-3′). The *6-OST-1* primer sequences are derived from the human *6-OST-1* cDNA sequence (from residues 240 to 264) and to the complement of this sequence (from residues 1147 to 1172) as reported (32). After 30 thermal cycles (1 min of denaturation at 94 °C, 2 min of annealing at 55 °C, 3 min of extension at 72 °C), the amplification products were analyzed in 1% agarose gels and detected by ethidium bromide staining. The amplification products were excised from the gel and cleaned by Gel Extraction kit (Qiagen). The PCR product was treated with *Bgl*II and *Xba*I, ligated into *Xba*I- and *Bam*HI-digested pInd/Hygro plasmid (CLONTECH), and transformed into *Escherichia coli* DH5α-competent cells. Four clones from each of two separate PCR reactions were sequenced and found to be identical. pInd/Hygro *6-OST-1*-containing plasmid was transfected into the CHO mutant cells. Cells positive for AT and FGF-2 binding were sorted and subsequently single-cell-cloned into a 96-well plate. The single-cell clones were expanded and frozen for further analysis.

6-O-Sulfation of HS in Vitro—The standard reaction mixture contained 50 mM MES (pH 7.0), 1% (w/v) Triton X-100, 5 mM $MnCl_2$, 5 mM $MgCl_2$, 2.5 mM $CaCl_2$, 0.075 mg/ml protamine chloride, 1.5 mg/ml bovine serum albumin, either metabolically labeled [^{35}S]HS or non-radioactive HS chains, cold PAPS (0.5 mM) or [^{35}S]PAPS (25 μM, 2×10^7 cpm), and 70 ng of purified baculovirus-expressed human *6-OST-1* in a final volume of 50 μl. The mixtures were incubated either 20 min or overnight at 37 °C, and 200 μg of chondroitin sulfate C was added. HS chains were purified by phenol/chloroform extraction and anion exchange chromatography on 0.25-ml columns of DEAE-Sephacel packed in 1-ml syringes (20). After ethanol precipitation, the pellets were washed with 75% ethanol, dried briefly under vacuum, and dissolved in water for further analysis.

Separation of HS^{act} and HS^{inact} by AT-affinity Chromatography—The procedure is identical to that described previously (29).

Disaccharide Analysis of HS—Heparitinase I (EC 4.2.2.8), heparitinase II (no EC number), and heparinase (EC 4.2.2.7) were obtained from Seikagaku, and heparitinase IV was a gift from Dr. Yoshida, Seikagaku Corp., Tokyo. Heparitinase I recognizes the sequences GlcNAc/NS±6S(3S?)-↓GlcUA/IdoUA-GlcNAc/NS±6S. The arrow indicates the cleavage site. Heparitinase II has broad sequence recognition: GlcNAc/NS±6S(3S?)-↓GlcUA/IdoUA±2S-GlcNAc/NS±6S. Heparinase (heparitinase III) and heparitinase IV recognize the sequences GlcNS±3S±6S-↓IdoUA2S/GlcUA2S-GlcNS±6S. The reaction products and references can be found in Refs. 33 and 34. The digestion of HS^{act} was carried out in 100 μl of 40 mM ammonium acetate (pH 7.0) containing 3.3 mM $CaCl_2$ with 1 milliunit (mU) of heparitinase I or 1 mU of each heparitinase I, heparitinase II, heparitinase IV, and hepa-

rinase (heparitinase III). The digestion was incubated at 37 °C overnight unless otherwise indicated.

For low pH nitrous acid degradation, radiolabeled HS samples were mixed with 10 μg of bovine kidney HS (ICN) and digested (35).

Disaccharides were purified by Bio-Gel P2 chromatography and resolved by ion pairing reverse-phase HPLC with appropriate disaccharide standards (36). Bio-Gel P2 or P6 columns (0.75 × 200 cm) were equilibrated with 100 mM ammonium bicarbonate. Radiolabeled samples (200 μl) were mixed with dextran blue (5 μg) and phenol red (5 μg) and loaded onto the column. The samples were eluted at a flow rate of 4 ml/h with collection of 0.5-ml fractions. The desired fractions were dried under vacuum, individually or pooled, to remove ammonium bicarbonate.

ΔUA-GlcNS3S Disaccharide Structure Determination by Capillary IPRP-HPLC Coupled with Mass Spectrometry—It has been reported that heparin molecules exhibiting a high affinity for a synthetic peptide (CRPKAKAKAKAKDQTK) mimicking a heparin-binding domain of heparin interacting protein (HIP) also show an extremely high affinity for AT (37). We expected that inclusion of this small peptide in the heparitinase digestion solution would protect 3-*O*-[^{35}S]sulfate-labeled HS from degrading into tetrasaccharide. Theoretically, we should recover HIP peptide-protected, AT-binding HS oligosaccharides. However, in the presence of the HIP peptide, all the 3-*O*-[^{35}S]sulfate-labeled sugars were degraded into disaccharides instead of oligosaccharides or tetrasaccharides as judged by their elution position on Bio-Gel P2 and their unique elution positions on IPRP-HPLC (the major 3-*O*-[^{35}S]sulfate-containing disaccharides eluted right before ΔUA-GlcNS6S disaccharide standard). Because there is no ΔUA-GlcNS3S standard reported, we decided to prove the structure. We first made stable isotope PAP^{34}S. The PAP^{34}S (99% isotope purity determined by ESI-MS) was prepared by incubating ATP and stable isotope $Na_2{}^{34}SO_4$ (Isonics Corp.) with ATP sulfurylase (Sigma Chemical Co.), adenosine 5′-phosphosulfate kinase (a generous gift from Dr. Irwin H. Segel), and inorganic pyrophosphatase (Sigma) (38). HS chains from wild-type CHO cells were labeled with pure 3-OST-1 plus PAP^{34}S. We then developed a capillary IPRP-HPLC (LC Packings) method for separating HS disaccharides, which is similar to a conventional IPRP-HPLC (29) except that 5 mM dibutylamine is used as an ion-pairing reagent (Sigma), and then coupled it to an electrospray ionization time-of-flight mass spectrometer (Mariner Workstation, PerSeptive Biosystems, Inc.) to detect the mass of each disaccharide eluted. Six HS disaccharide standards from Seikagaku were separated by capillary HPLC and detected by negative polarity ESI-MS. The accuracy of the ESI-MS is ± 0.001 *m/z* unit after calibration with the molecular standard sets supplied by the manufacture (bis-trifluorobenzoic acid, heptadecafluorononanoic acid, perfluorotetradecanoic acid). 3-*O*-^{34}S-labeled HS was digested with a combination of 1 mU of each heparitinase I, heparitinase II, heparitinase IV, and heparinase in the absence or presence of 0.5 mg/ml HIP peptide. 0.5 μg of digested HS was injected into capillary HPLC coupled with mass spectrometry (see Fig. 3). UV *peak B* eluted at the same time as a ΔUA-GlcNS6S standard, whereas UV *peak D* eluted at the same time as a ΔUA2S-GlcNS standard (see Fig. 3*A*). Three major ions with *m/z* 247.5, 496.0, and 625.2 were observed in both UV peaks (see Fig. 3, *panels B* and *D*), where 496.0 is z1 (−1)-charged, 247.5 is z2 (−2)-charged, and 625.2 is one dibutylamine-adducted with z1 (−1)-charged ΔUA-GlcNS6S or ΔUA2S-GlcNS disaccharides. However, when the *m/z* region 494.0–501.0 from both *peaks B* and *D* were expended (*panels C* and *E*), a non-natural abundant, z1-charged molecular ion with *m/z* 498.0 was observed in UV *peak B* but not in UV *peak D*. 498.0 *versus* 496.0 of disaccharide ions should represent ΔUA-GlcNS3[^{34}S]S and ΔUA-GlcNS6S, respectively. The mass for ΔUA-GlcNS3[^{34}S]S was barely detectable in the absence of HIP peptide, which is consistent with the literature that 3-*O*-sulfate-containing sugars are usually degraded into tetrasaccharides, not disaccharides, by a mixture of heparitinase digestion (20, 33). Therefore, HIP peptide is included in heparitinase digestion when we degrade 3-*O*-containing HS into disaccharides.

Northern Blot Hybridization and RT-PCR—To generate specific Northern blot hybridization probes, PCR primers were designed that bracket unique sequences within human 6-OST-1, 6-OST-2 and 6-OST-3. A 249-bp PCR product that corresponds to a region within the 3′-UTR of the *6-OST-1* gene starting at position 1772 and ending at 2021 was used as an isoform specific probe. Similarly, a 299-bp PCR product that corresponds to a region in the 3′-UTR of the 6-OST-2 gene starting at position 1831 and ending at 2130, and another product within the 3′-UTR of the *6-OST-3* gene starting at 943 and ending at 1378 (444 bp) were used as a probe. PCR was performed with [α-^{32}P]dCTP (PerkinElmer Life Sciences), and isoform-specific radiolabeled probes were purified on G-25 Sephadex spin columns (Roche Molecular Biochemicals). Hybridizations were carried out according to the manufacturer's instructions using 2×10^6 cpm probe per milliliter of ExpressHyb solution (CLONTECH). After the hybridizations were complete, the blots were washed twice in 2× SSC containing 0.1% SDS and once with 0.1× SSC containing 0.1% SDS, all at room temperature. Blots were then washed with 0.1× SSC containing 0.1% SDS at 50 °C. For blots hybridized with the *6-OST-1* probe, this last wash was repeated twice at 65 °C. The membranes were then subjected to autoradiography with BioMax imaging film (Kodak) with a BioMax MS intensifying screen (Kodak).

For RT-PCR, poly(A)-purified or DNase I-treated total RNA was used. Primer pairs were designed that bracket isoform-specific regions within the human sequences for both *6-OST-2* and *6-OST-3*. For *6-OST-1*, a 569-bp fragment corresponding to nt 54 (GCG TGC TTC ATG CTC ATC CT) to 622 (GTG CGC CCA TCA CAC ATG T) within the hamster sequence was used. For *6-OST-2*, PCR targets included regions starting at nt 23 (CTG CTG CTG GCT TTG GTG AT) and 346 (GCA GAA GAA ATG CAC TTG CCA) and ending at nt 1471 (GCC GCT ATC ACC TTG TCC CT), 1491 (TCA TTG GTG CCA TTG CTG G), and 1532 (TGA GTG CCA GTT AGC GCC A). For 6-OST-3, the targets included regions that start at nt 5 (CCG GTG CTC ACT TTC CTC TTC) and 353 (TTC ACC CTC AAG GAC CTG ACC) and end at nt 988 (GCT CTG CAG CAG GAT GGT GT) and 1217 (GCT GGA AGA GAT CCT TCG CAT AC). Total RNA was purified from wild-type and mutant CHO-K1 cells using the RNeasy total RNA kit from Qiagen according to the manufacturer's instructions. RNA was quantitated by absorbance at 260 nm, and 100 μg of total RNA was reacted with DNase I (Ambion) at 37 °C for 45 min, twice extracted with equal volumes of acid phenol/chloroform, precipitated in ethanol, and reconstituted in diethyl pyrocarbonate-treated water. Further selection of poly(A) plus RNA was carried out with the Oligotex mRNA kit (Qiagen). RNA integrity was checked after electrophoresis on a 1% agarose gel, and all RT reactions were run with Moloney murine leukemia virus reverse transcriptase (Ambion) according to manufacturer's instructions. PCR was performed with Super *Taq* polymerase (Ambion).

Baculovirus Expression and Purification of 6-OST-1—Human 6-OST-1 recombinant baculovirus was prepared using the pFastBas HT donor plasmid modified by the insertion of honeybee mellitin signal peptide (36) and the Bac-to-Bac baculovirus expression system (Life Technologies, Inc.) according to the manufacturer's protocol, except that recombinant bacmid DNA was purified using an endotoxin-free plasmid purification kit (Qiagen, Inc.) and transfection of Sf9 cells was scaled up to employ 3 μg of bacmid DNA and 6×10^6 exponentially growing cells in a 100-mm dish. At day 3 post-transfection, baculovirus was precipitated from the medium with 10% polyethylene glycol, 0.5 M NaCl at 12,000 × *g*, re-suspended in 14 ml of medium, and applied to a 100-mm dish seeded with 1.5×10^7 Sf9 cells. Medium from the infected cells was harvested after 90 h of growth at 27 °C, centrifuged at 400 × *g*, made to 10 mM in Tris, adjusted to pH 8.0, and centrifuged at 4000 × *g*. Clarified medium was diluted with an equal volume of cold 10 mM Tris-HCl, pH 8.0, and stirred for 30 min with 0.6 ml (packed volume) of Toyopearl 650M chromatographic media (TosoHaas). The heparin-Sepharose was packed into a column (0.4 × 4.75 cm), washed with 5 ml of TCG 50 (10 mM Tris-HCl, pH 8.0, 2% glycerol, 0.6% CHAPS, 50 mM NaCl), eluted with 1.2 ml of TCG 1000 (as above, but 1 M in NaCl) containing 10 mM imidazole, and concentrated to 0.25 ml in a Microcon YM-10 centrifugal filter (Millipore Corp.).

Histidine-tagged recombinant *6-OST-1* was affinity-purified by mixing the product eluted from heparin-Sepharose for 90 min at 4 °C with nickel-nitrilotriacetic acid magnetic agarose beads (Qiagen, Inc.) magnetically sedimented from 60 μl of suspension. The beads were washed twice with 0.125 ml of TCG 400 containing 20 mM imidazole and eluted twice with 0.03 ml of TCG 400 containing 250 mM imidazole. The combined elution fractions contained ~25% of the sulfotransferase activity present in the starting medium.

Bacterial Expression and Purification of 6-OST-1—Expression vector pET15b was purchased from Novagen (Madison, WI). *E. coli* strains BL21 and DH5α were obtained through the ATCC (Manassas, VA). An *Ase*I restriction site was introduced at 211–216 bp, and a *Bam*HI restriction site was introduced at 1344–1349 bp of human 6-OST-1 (32) by PCR. The *6-OST-1* gene was then ligated into *Nde*I- and *Bam*HI-digested pET15b and transformed into competent *E. coli* strain DH5α. A BL21 colony containing 6-OST-1 in pET15b with confirmed sequence was used to inoculate 2 liters of LB containing 100 μg/ml ampicillin. The cultures were shaken in flasks at 250 rpm at 37 °C. When the optical density at 600 nm reached 1.2, 1 mM isopropyl-1-thio-β-D-galactopyranoside was added to the cultures. The cultures were then agi-

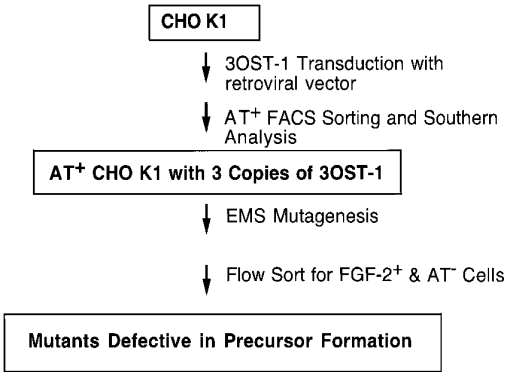

FIG. 1. **Scheme for making mutants.** Using recombinant retroviral transduction, the human HS 3-*O*-sulfotransferase 1 (*3-OST-1*) gene was transduced into CHO cells. *3-OST-1* expression gives rise to CHO cells with the ability to produce anticoagulant HS (HS^{act}). A cell line that has three copies of *3-OST-1* was chosen by Southern analysis. After chemical mutagenesis of this cell line, FGF-2 binding-positive and AT binding-negative mutant cells were FACS-sorted and cloned. The advantage of having three copies of *3-OST-1* is that upstream genes that are responsible for generating specific HS precursor structures can be sought after chemical mutagenesis without losing *3-OST-1*. FGF-2 selection is employed to make certain that the mutant cells still make HS.

tated at 250 rpm overnight at room temperature. The cells were pelleted at 5000 rpm for 15 min. The supernatant was discarded, and the cell pellet was resuspended in 40 ml of 20 mM Tris, 500 mM NaCl, 0.6% CHAPS, 1% glycerol, and 5 mM imidazole, pH 7.9 ("binding buffer"). The cells were homogenized, and the homogenate was centrifuged at 13,000 rpm for 20 min. The supernatant was filtered through 0.2-μm filter paper and loaded onto a BioCAD HPLC system (PerSeptive Biosystems, Cambridge, MA) and purified using Ni^{2+} chelate chromatography. Briefly, the supernatant was loaded onto the column and washed with binding buffer until unbound material was washed off the column. Then, low affinity material was washed off the column using 20 mM Tris, 500 mM NaCl, 0.6% CHAPS, 1% glycerol, and 55 mM imidazole, pH 7.9, and *6-OST-1* was eluted from the column with 20 mM Tris, 500 mM NaCl, 0.6% CHAPS, 1% glycerol, and 500 mM imidazole, pH 7.9. The purity of the recombinant *6-OST-1* was determined using a silver-stained protein gel.

RESULTS

Similar Charge Density in GAGs from HS^{act} Defective Mutant and Wild-type Cells—The interaction of AT with heparin/HS depends on a pentasaccharide sequence consisting of GlcNAc/NS**6S**-GlcUA-GlcNS**3S**±6S-IdoUA2S-GlcNS6S, where the **3S** and **6S** groups constitute the most critical elements involved in the interaction. We reasoned that mutant cells, which make HS lacking the critical **6S** group or having an improper *N*-sulfation/epimerization pattern that fails to generate HS^{act} precursor, should not bind to AT. By using the scheme shown in Fig. 1, we obtained cell mutants that are defective in AT-binding (Fig. 2*B*). We first examined the synthesis of GAGs in the HS^{act}-defective mutant by biosynthetic labeling studies with [6-^{3}H]GlcN (Fig. 3). HPLC anion-exchange analysis of the [^{3}H]GAG chains from the mutant cells resolved HS (0.31–0.50 M NaCl) from chondroitin sulfate (0.52–0.60 M NaCl) (Fig. 4, *solid tracer*). The GAG chains from the *3-OST-1*-expressing wild-type resolved into a similar profile to that of the mutant (Fig. 4, *broken tracer*). This finding implies that the HS from the mutant has a similar charge density to that of the wild-type.

HS^{act}-defective Mutant Makes Less 6-O-Sulfate-containing Disaccharides—Because HS from the mutant has similar charge density to that of the wild-type, the decrease in AT binding in the mutant should correlate with a change in the structure of the HS chains.

We checked the synthesis of GAGs in the mutant by biosynthetic labeling studies with [^{35}S]sulfate. The *3-OST-1*-expressing wild-type and mutant cells produced the same amount of [^{35}S]HS and contained ~70% HS and ~30% chondroitin sulfate (data not shown), which is consistent with the result shown in Fig. 4 (68% of HS in the mutant *versus* 66% of HS in the *3-OST-1*-expressing wild-type). [^{35}S]Sulfate-labeled HS chains from the 3-OST-1-expressing wild-type and mutant cells were then digested with a mixture of heparitinases. The resulting disaccharides (~93% of total [^{35}S]sulfate counts) were separated on a Bio-Gel P2 column and then further resolved by IPRP-HPLC with appropriate internal standards (Table I). The mutant cells make decreased amounts of 6-*O*-sulfated disaccharides, including ΔUA-GlcNAc6S, ΔUA-GlcNS6S, and ΔUA2S-GlcNS6S (Table I).

HS^{act}-defective Mutant and Wild-type CHO Cells Express 6-OST-1 but Not 6-OST-2 and 6-OST-3 mRNA—To explain the reduced levels of 6-*O*-sulfate-containing disaccharides in the mutant, we first checked how many *6-OST* isoforms are expressed in CHO wild-type *versus* mutant cells. Three murine *6-OST* isoforms have been cloned (2). We have cloned and used human *6-OST-1*, *6-OST-2*, and *6-OST-3* cDNA as probes and conducted both Northern and RT-PCR studies in the mutant and the *3-OST-1*-expressing wild-type CHO cells. Northern analysis indicates that the mutant and the *3-OST-1*-expressing wild-type have the same level of *6-OST-1* mRNA. No *6-OST-2* and *6-OST-3* mRNA was detected on the same blot (data not shown). These results suggest that CHO cells might only express *6-OST-1*. To prove this, one set of PCR primers for *6-OST-1*, three sets of PCR primers for *6-OST-2*, and two sets of PCR primers for *6-OST-3* were made and RT-PCR reactions were conducted using wild-type and mutant mRNA as templates (see "Experimental Procedures"). The same level of *6-OST-1* PCR products was observed for both wild-type and the mutant, but no amplification was observed for three sets of *6-OST-2* and two sets of *6-OST-3* RT-PCR reactions. These results confirm the Northern analysis that CHO cells express *6-OST-1*, but not *6-OST-2* and *6-OST-3*.

HS^{act}-defective Mutant Does Not Contain a Point Mutation in 6-OST-1 Coding Region—Because Northern and RT-PCR analyses indicate that the mutant and wild-type have the same level of *6-OST-1*, this observation raises the possibility that the mutant might have point mutation(s) in the *6-OST-1* amino acid coding region that cause decreased 6-*O*-sulfotransferase activities. The coding regions of *6-OST-1* RT-PCR products from the mutant were double-strand-sequenced. No point mutation was observed compared with wild-type (data not shown).

HS^{act}-defective Mutant Has Decreased 6-O-Sulfotransferase Activities—The mutant cells are defective in AT binding (Fig. 2*E*). Disaccharide compositional studies indicate that the mutant makes less 6-*O*-sulfated residues (Table I); however, there was no change in either the level of mRNA expression nor the mutation of the coding sequence of *6-OST-1* (data not shown). These results suggest that the mutant might have a defect in *6-OST-1* activities. To test this hypothesis, sulfotransferase activity assays were conducted using HS from wild-type CHO cells, *N*-, *O*-desulfated, re-*N*-sulfated heparin (CDSNS-heparin) and 6-*O*-desulfated heparin (a generous gift from Dr. Jeffrey D. Esko) as substrates and crude cell homogenates from wild-type and mutant CHO cells as a source of enzyme. In the wild-type, enzyme activity was proportional to time for ~2 h and with the amount of cell protein added up to100 μg. The reaction products were digested by a combination of heparitinase digestion, followed by Bio-Gel P2 chromatography. The disaccharides collected were subjected to IPRP-HPLC analysis. Both 2-*O*-[^{35}S]sulfate- and 6-*O*-[^{35}S]sulfate-labeled disaccharides were quantitated in both the *3-OST-1*-expressing wild-

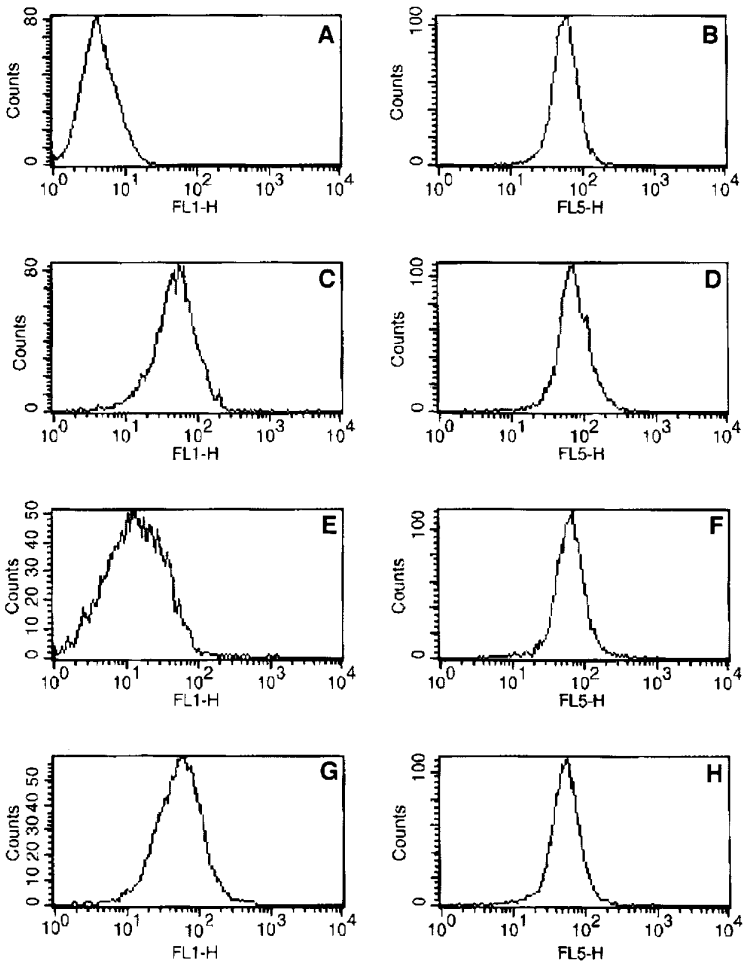

FIG. 2. **Dual-color fluorescence flow cytometric analysis of AT (*A*, *C*, *E*, and *G*) and FGF-2 (*B*, *D*, *F*, and *H*) binding to wild-type, mutant, and *6-OST-1* correctant.** CHO wild-type (*A* and *B*); wild-type CHO cell clone with three copies of *3-OST-1* (*C* and *D*), mutant cell clone with three copies of *3-OST-1* (*E* and *F*), and *6-OST-1* correctant of the mutant (*G* and *H*) were double-labeled with fluorescein-AT (*A*, *C*, *E*, and *G*) and Alexa 594-FGF-2 (*B*, *D*, *F*, and *H*) and subjected to dual-color FACS ("Experimental Procedures").

type and mutants. 2-*O*-Sulfotransferase activity was similar in mutant cells (118 ± 3 pmol/min/mg) and the wild-type cells (122 ± 2 pmol/min/mg) when CDSNS-heparin was used as substrate. However, 30–39% reduction of 6-*O*-sulfotransferase activities in the mutant was observed with all three substrates (Table II).

In Vivo 6-OST-1-corrected Mutant (Correctant) Makes HS, 50% of Which Is HS^{act}—Decreased *6-OST-1* activity in the mutant might be responsible for its deficiency in AT binding. To test this idea, the CHO *6-OST-1* coding region was successfully amplified and sequenced from the CHO-K1 quick-clone cDNA library by PCR, because only partial 6-OST-1 coding sequence from CHO cells has been reported (32). The CHO *6-OST-1* sequence has been deposited in GenBank™ (accession number AB006180; the differences in the amino acid residues from the previously reported partial sequence of the same cDNA (32) are commented upon). CHO *6-OST-1* cDNA was then expressed in the mutant. The stable transfectants were labeled with fluorescein-AT and Alexa 594-FGF-2 and subjected to dual-color FACS. The correctants with high AT binding affinity were single-cell-cloned (Fig. 2*G*). [^{35}S]Sulfate metabolically labeled HS from correctants was isolated. AT-affinity chromatography of [^{35}S]HS indicates that the correctant makes 50% HS^{act} chain. This represents the highest percentage of HS^{act} production by any cell lines reported so far. We then analyzed the disaccharide composition of the correctant cells. [^{35}S]Sulfate metabolically labeled HS from *3-OST-1* expression wild-type, mutant, and correctant cell clones were isolated and digested with a mixture of heparitinases. The resulting disaccharides were separated on a Bio-Gel P2 column and were then further resolved by IPRP-HPLC (Fig. 4). The correctant exhibited a greatly increased amount of both GlcNAc6S (9% *versus* 5%) and GlcNS6S (13% *versus* 4%) residues compared with the mutant. The amount of GlcNAc6S and GlcNS6S residues in the correctant cells exceeded the amount of GlcNAc6S and GlcNS6S residues in the wild-type CHO-K1 cells with three copies of *3-OST-1* (GlcNAc6S (9% *versus* 7%) and GlcNS6S (13% *versus* 9%)) (Table I).

In Vitro 6-OST-1 Sulfation Generates Three Kinds of 6-O-containing Disaccharides—To explain the difference between *6-OST-1* substrate specificity observed *in vivo* and the published data (2), we expressed and purified *6-OST-1* in bacteria and baculovirus. [^{35}S]Sulfate metabolic-labeled mutant HS chains were treated with baculovirus-expressed pure *3-OST-1*, *6-OST-1*, or both plus cold PAPS and AT-affinity purified. HS^{act} was isolated and HS^{act}% was quantitated (Table III). For the HS chain from mutant, *3-OST-1* modification alone increases HS^{act}% from 7% to 12%, *6-OST-1* modification alone increases HS^{act}% from 7% to 51%, both *3-OST-1* and *6-OST-1* modification increases HS^{act}% from 7% to 64%. For the HS chain from wild-type with three copies of *3-OST-1* genes, *3-OST-1* modification alone increases HS^{act}% from 26% to 40%, 6-OST-1 modification alone increases HS^{act}% from 26% to 64%, both *3-OST-1* and *6-OST-1* modification increases HS^{act}% from 26% to 70%. These results indicate both *3-OST-1* and *6-OST-1* are critical enzymes involved in HS^{act} production. The yield of

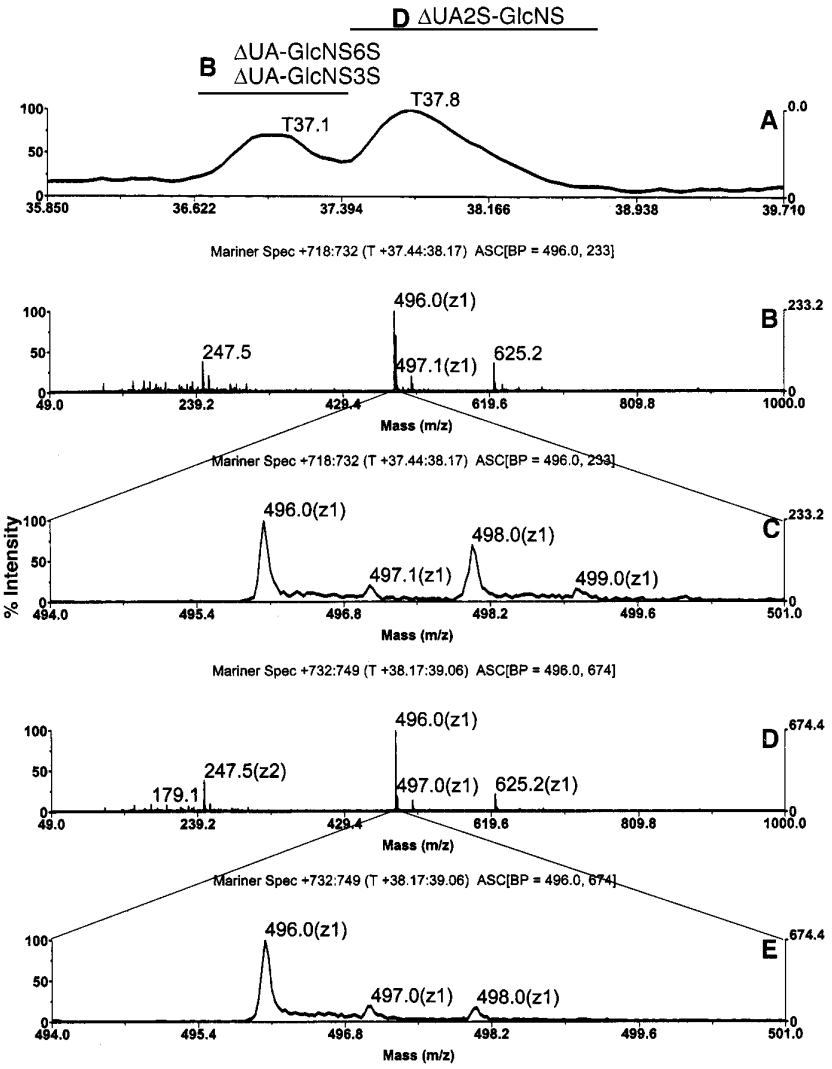

FIG. 3. **ΔUA-GlcNS3S disaccharide structure determination by capillary IPRP-HPLC coupled with mass spectrometry.** Cold HS-chain form wild-type CHO cells were labeled with *3-OST-1* plus PAP[34]S. Purified HS was digested with a combination of 1 mU of each heparitinase I, heparitinase II, heparitinase IV, and heparinase in the presence of 0.5 mg/ml heparin/heparan sulfate interacting protein (HIP) peptide. 0.5 μg of digested HS was injected into capillary IPRP-HPLC coupled with MS. *A*, UV tracer of capillary IPRP-HPLC from 35.85 to 39.71 min; *peak B* contains both ΔUA-GlcNS6S and ΔUA-GlcNS3S, and *peak D* contains ΔUA2S-GlcNS; *B*, negative polarity MS spectra from 37.44 to 38.17 min, which equals the UV peak from 36.64 to 37.37 min; *C*, amplification of the *m/z* 494.0–501.0 region from *panel B*; *D*, negative polarity MS spectra from 38.17 to 39.06 min, which equals the UV peak from 37.37 to 38.26 min; *E*, amplification of the *m/z* 494.0–501.0 region from *panel D*.

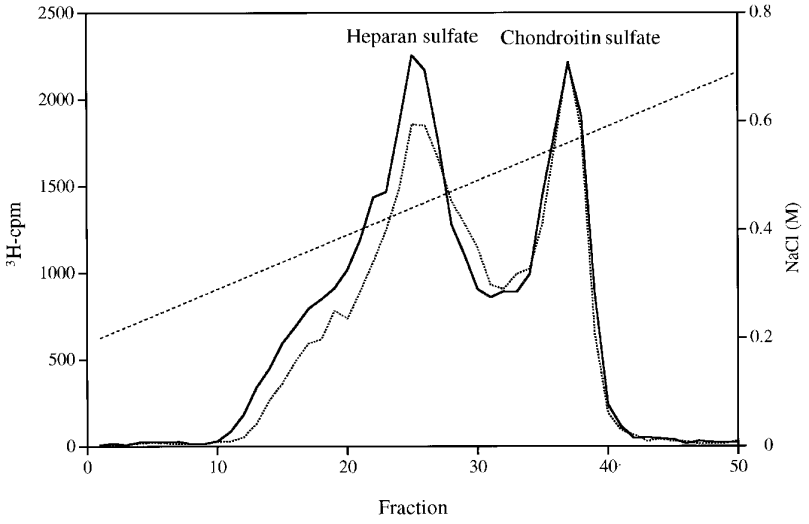

FIG. 4. **HPLC anion-exchange chromatography of GAGs.** [^{3}H]GlcN-labeled GAG chains from wild-type and mutant were isolated by protease digestion and β-elimination (see "Experimental Procedures"). Samples were analyzed by HPLC anion-exchange chromatography (see "Experimental Procedures"). *Solid tracer*, mutant; *broken tracer*, wild-type. The *broken line* indicates the concentration gradient of sodium chloride.

HS^{act} by *6-OST-1* treatment of mutant HS chain is similar to that of the wild-type even though 6-*O*-sulfation is severely decreased in the mutant (Table I, Fig. 5). To locate where *6-OST-1* adds 6S residues along the HS chains, equal amounts of HS from *3-OST-1*-expressing wild-type and mutant cells were *in vitro* labeled with purified baculovirus expressed

TABLE I
Disaccharide composition of HS from mutant, wild-type, and 6-OST-1 correctant cells

[^{35}S]Sulfate metabolicly labeled HSs from *3-OST-1*-expressing wild-type, mutant, and *6-OST-1* correctant cells were isolated and digested with a mixture of heparitinases. The resulting disaccharides were separated on a Bio-Gel P2 column and were then further resolved by IPRP-HPLC with appropriate internal standards. In duplicate experiments, the values varied by ≤20% of those shown.

Name	Mutant	Wild-type	Correctant
		%	
ΔUA-GlcNS	35	30	27
ΔUA-GlcNAc6S	5	7	9
ΔUA-GlcNS6S	4	9	13
ΔUA2S-GlcNS	36	20	22
ΔUA2S-GlcNS6S	19	34	29

6-OST-1 and [^{35}S]PAPS either for 20 min or overnight. Only ~1/3 as much radioactivity was incorporated into wild-type HS as compared with the mutant. [^{35}S]Sulfate-labeled HSs were isolated and digested with a mixture of heparitinases. The resulting disaccharides (~94% of [^{35}S]sulfate counts) were separated on a Bio-Gel P2 column and were then further resolved by IPRP-HPLC with appropriate internal standards (Fig. 6, mutant, *solid tracer*; wild-type, *broken tracer*). Indeed, *6-OST-1* not only adds a 6S group on GlcNS but also on GlcNAc residues in both wild-type and mutant HS. Much more ΔUA-GlcNAc6^{35}S and ΔUA-GlcNS6^{35}S disaccharides were observed from reactions run overnight than after just 20 min (6^{35}S-sulfate distribution in ΔUA-GlcNAc6^{35}S, ΔUA-GlcNS6^{35}S, and ΔUA2S-GlcNS6^{35}S = 29%, 18%, and 53% for overnight labeling *versus* 18%, 12%, and 70% for 20-min labeling in the mutant). We noticed that the 6-*O*-sulfate incorporation was 10 times higher from baculovirus-expressed *6-OST-1* than bacteria-expressed *6-OST-1* when the same amount of *6-OST-1* protein and mutant HS was used. However, three 6-*O*-sulfated disaccharides generated by bacterial *6-OST-1* with overnight labeling had the ratio, ΔUA-GlcNAc**6**^{35}**S** (25%), ΔUA-GlcNS**6**^{35}**S** (20%), and ΔUA2S-GlcNS**6**^{35}**S** (55%), and is very similar to that observed in baculovirus *6-OST-1* overnight-labeled disaccharides (Fig. 6*B*).

Contribution of 6-OST-1 in Generating HS^{act} Oligosaccharides—To further locate the 6-*O*-sulfate addition in AT-binding HS^{act} oligosaccharides, cold mutant HS chains were treated with purified baculovirus-expressed 6-OST-1 with [^{35}S]PAPS overnight. After heparitinase I digestion, HS^{act} oligosaccharides were affinity-purified (7% of 6-*O*-[^{35}S]sulfate-labeled HS^{total}). The HS^{act} oligosaccharides were then treated with low pH nitrous acid that cleaves *N*-sulfated residues, and a combination of heparitinases that cleaves 3-*O*-sulfate-containing sugar into tetrasaccharides and all other sugars into disaccharides. Treated and untreated HS^{act} oligosaccharides were run on Bio-Gel P6 columns (Fig. 7). Di- and tetrasaccharides were collected from enzyme and low pH nitrous-treated samples as indicated. The tetrasaccharides resistant to a combination of heparitinases I and II and heparinase digestion represented the 3-*O*-sulfate-containing tetrasaccharides as reported earlier (20, 33). The presence of similar amounts of tetrasaccharides from both nitrous and enzyme degradation suggests the 3-*O*-containing tetrasaccharides have the structures, UA±2S-GlcNAc**6**^{35}**S**-GlcUA-GlcNS3S±**6**^{35}**S**. To prove this, the tetrasaccharides (Fig. 8*A*) collected from enzyme digestion (Fig. 7*C*) were further digested into disaccharides (Fig. 8*B*) with heparitinase I in the presence of HIP peptide (the same method as shown in Fig. 3). IPRP-HPLC profiles of 6-*O*-sulfate-tagged HS^{act} di- and tetrasaccharides from Fig. 7*C* were shown in Fig. 8. Table IV summarizes the 6-*O*-[^{35}S]sulfate-labeled disaccharide compositions calculated based on the HPLC data (Fig. 8). In HS^{act} oligosaccharides, *6-OST-1* adds 6-*O*-sulfates not only at GlcUA/IdoUA-GlcNS, GlcUA-GlcNAc, and IdoUA2S-GlcNS, but also at GlcUA-GlcNS3S. These results show that *6-OST-1* is the enzyme that not only puts the critical 6-*O*-sulfate group in HS^{act} oligosaccharides but also other 6-*O*-sulfate groups in HS^{act} oligosaccharides as well. *3-OST-1* and *6-OST-1* are, therefore, the critical enzymes for the generation of HS^{act}.

TABLE II
Decreased 6-OST-1 activities in HS^{act} defective mutant

Sulfotransferase activities were assayed using three different substrates and crude cell homogenates from wild-type and mutant CHO cells as a source of enzyme.

Substrates	6-*O*-sulfotransferase activities	
	Wild-type	Mutant
	pmol/min/mg	
HS (CHO-K1)	5.6 ± 0.3	3.9 ± 0.4 (70%)[a]
6-*O*-Desulfated heparin	4.4 ± 0.3	2.7 ± 0.5 (61%)
CDSNS-heparin	11 ± 2	7 ± 1 (62%)

[a] Numbers in parentheses represent percentage of wild-type activity.

TABLE III
6-OST-1 limits the anticoagulant HS generation

Treated with baculovirus-expressed pure *3-OST-1*, *6-OST-1*, or both plus cold PAPS, the modified [^{35}S]sulfate metabolic-labeled mutant and wild-type HS chains were AT-affinity purified. HS^{act} was isolated and HS^{act}% was quantitated. In different experiments, the values varied by ≤2% of those shown.

	Control	[^{35}S]HS^{act}%		
		+3-OST-1	+6-OST-1	+3&6-OST-1
		%		
Mutant	7	12	51	64
Wild-type	26	40	64	70

DISCUSSION

A new approach for generating HS^{act} biosynthetic mutants and a novel method for characterizing 6-*O*-sulfotransferase substrate specificity have been developed in this study. This approach includes placing multiple copies of a downstream enzyme into CHO cells and then mutagenizing these cells. Mutants defective in upstream enzymes that are part of the anticoagulant HS biosynthetic pathway were then sorted by FACS. A mutant was then characterized both *in vivo* and *in vitro* to delineate enzymes involved in generating anticoagulant HS. The advantage of sorting is that it targets GAG synthesis selectively and very large populations of cells can be screened, which make it possible to detect specific mutations in effecting distinct HS structures. This technique may constitute a general approach for defining, obtaining, and characterizing the components of a biosynthetic pathway once the terminal biosynthetic enzyme is obtained and proteins that recognize the final product of the pathway are available.

It has been reported that a type of size exclusion chromatography coupled with mass spectrometry is effective for compositional analysis of chondroitin sulfate oligosaccharides. Mass spectrometric detection produces far more information than conventional UV or fluorescent detectors and allows the monosaccharide composition of individual components to be determined (39). Introducing the stable isotope PAP^{34}S into the 3-*O* position of HS by pure *3-OST-1* as described in Fig. 3, a 3-*O*-sulfate-containing disaccharide with a unique mass, which has not been reported before, was readily identified by a combination of capillary IPRP-HPLC coupled with mass spectrometry. The method developed in this paper consumes 0.5 μg of total HS for separating and detecting different HS disaccharides. It will serve as a practical way of accomplishing HS disaccharide analysis of general HS samples from cells or tissues without radioisotope labeling. Furthermore, we could treat biologically

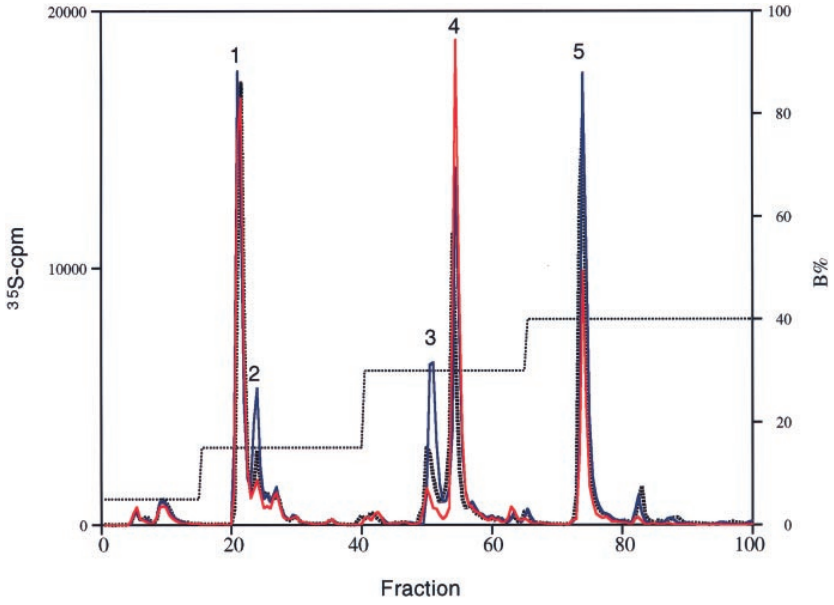

FIG. 5. **IPRP-HPLC of [^{35}S]sulfate metabolic-labeled HS disaccharides.** [^{35}S]Sulfate metabolically labeled HS from parental wild-type, mutant, and correctant were isolated and digested with a mixture of heparitinases. The resulting disaccharides were separated on a Bio-Gel P2 column and were then further resolved by IPRP-HPLC with appropriate internal standards. *1*, ΔUA-GlcNS; *2*, ΔUA-GlcNAc6S; *3*, ΔUA-GlcNS6S; *4*, ΔUA2S-GlcNS; and *5*, ΔUA2S-GlcNS6S. *Blue tracer*, mutant; *red tracer*, correctant; *black broken tracer*, wild-type. The *broken line* indicates the gradient of acetonitrile.

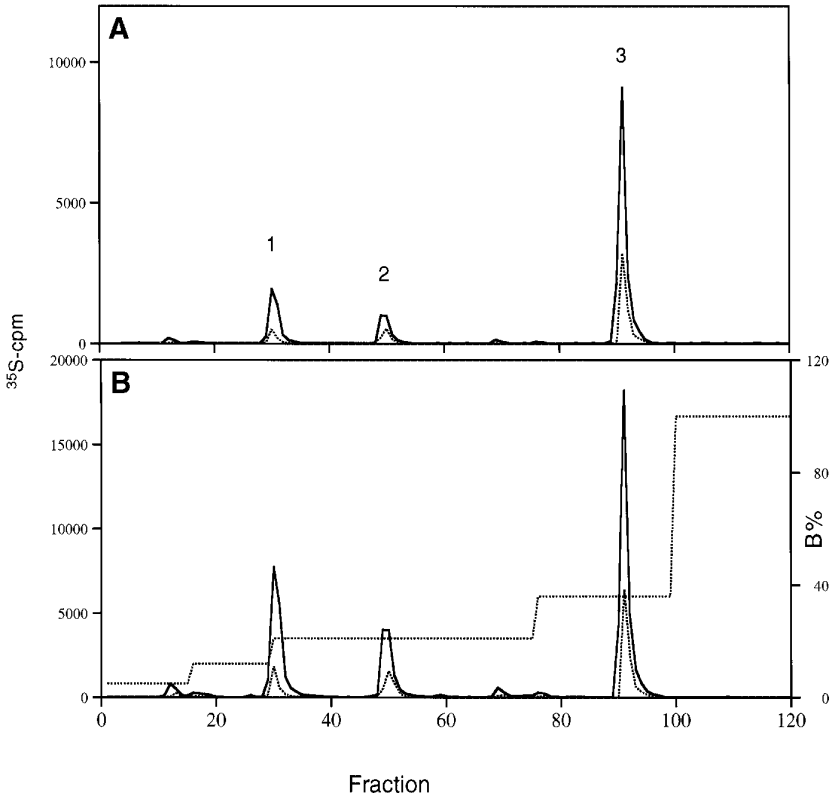

FIG. 6. **IPRP-HPLC of *6-OST-1* and [^{35}S]PAPS-labeled HS disaccharides.** Cold HS from *3-OST-1*-expressing CHO wild-type and mutant were *in vitro* labeled with purified baculovirus-expressed *6-OST-1* and [^{35}S]PAPS for 20 min (*A*) or overnight (*B*). [^{35}S]Sulfate-labeled HSs were isolated and digested with a mixture of heparitinases. The resulting disaccharides were separated on a Bio-Gel P2 column and were then further resolved by IPRP-HPLC with appropriate internal standards. *1*, ΔUA-GlcNAc6S; *2*, ΔUA-GlcNS6S; *3*, ΔUA2S-GlcNS6S. *Solid tracer*, mutant; *broken tracer*, wild-type. The *broken line* indicates the gradient of acetonitrile.

inactive HS oligosaccharides *in vitro* with different pure sulfotransferases plus stable sulfur isotopes of PAPS (PAP^{33}S and PAP^{34}S). Labeled oligosaccharides should regain biological function. The different stable isotope-tagged, biologically active oligosaccharides could then be sequenced by a combination of capillary IPRP-HPLC for separation and mass spectrometry for detection. In this manner, biologically critical regions can be pinpointed and sequenced.

Because *in vitro* 3-*O*-sulfation can transform anticoagulantly inactive HS chain into anticoagulantly active HS chain, it has been concluded that 3-*O*-sulfation is the final modification step during HS biosynthesis. This study shows *in vitro* 6-*O*-sulfation can transform 3-*O*-sulfate-containing anticoagulant inactive HS chain into anticoagulant active HS chain as well. It shows that it is still unclear whether 6-*O*-sulfation occurs before or after 3-*O*-sulfation during biosynthesis.

Three *6-OST* genes have been cloned and shown to be expressed in a tissue-specific pattern. Furthermore, the individual isozymes appear to differ in substrate specificity. We do not know how *6-OST-2* and *6-OST-3* contribute in HS^{act} generation *in vivo*. However, by comparing baculovirus-expressed and purified human *6-OST-1*, *6-OST-2*, and *6-OST-3*, we found

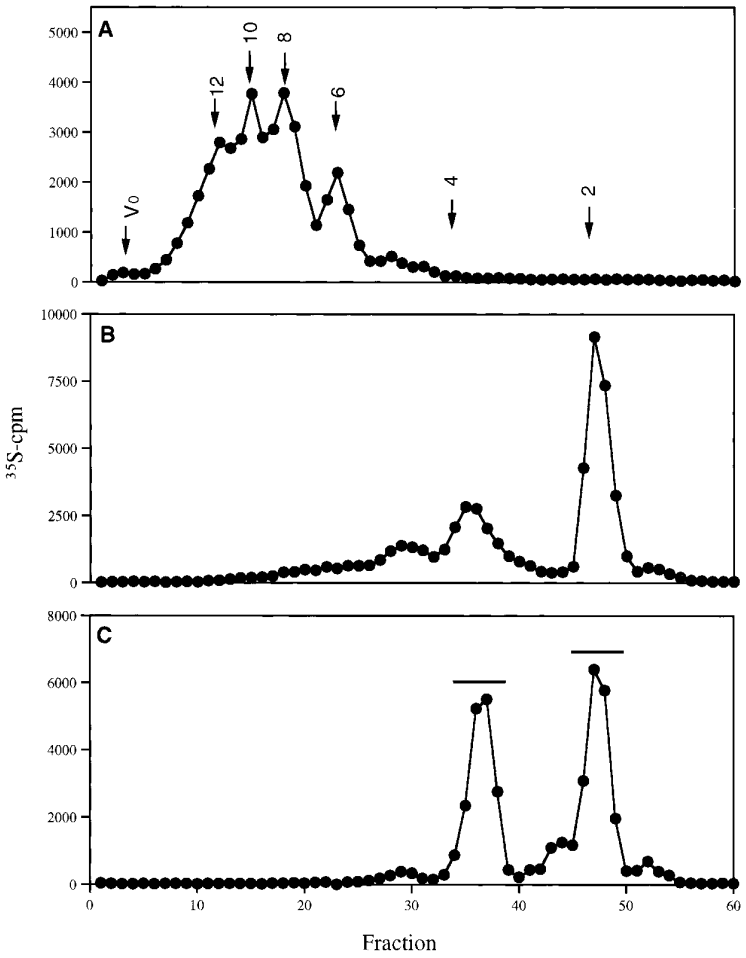

FIG. 7. **Bio-Gel P6 fractionation of digested HS.** 6-*O*-[^{35}S]Sulfate-tagged [^{3}H]HS from mutant were digested with 1 mU of heparitinase I for 1 h. HS^{act} oligosaccharides were obtained by AT-affinity chromatography (see "Experimental Procedures"). HS^{act} oligosaccharides were treated with low pH nitrous acid and then either $NaBH_4$-reduced or treated with heparitinase I, II, and heparinase was analyzed by Bio-Gel P6 chromatography ("Experimental Procedures"). The fractions indicated were pooled for further analysis. *A*, 6-*O*-[^{35}S]sulfate-tagged mutant HS^{act} oligosaccharides; *B*, 6-*O*-[^{35}S]sulfate-tagged mutant HS^{act} oligosaccharides treated with low pH nitrous acid and $NaBH_4$; *C*, 6-*O*-[^{35}S]sulfate-tagged mutant HS^{act} oligosaccharides digested with heparitinases. *n* = the number of monosaccharide units in each peak.

6-OST-1 is the most potent enzyme in generating HS^{act} by the *in vitro* assay we describe in this report.[2]

It has been shown that the critical 6-*O*- and 3-*O*-sulfates in HS^{act} oligosaccharides function in a thermodynamically linked fashion and work as a pincer in terms of AT binding. Previously we showed that there were multiple 3-*O*-sulfation sites in F9 HS^{act} and that 3-*O*-sulfates are either added to all the sites or none of the sites. In other words, *3-OST-1* works in a processive mode during biosynthesis by an unknown mechanism. Because CHO wild-type makes HS^{act} precursor with the critical 6S in the absence of *3-OST-1* and the mutant makes HS^{act} precursor with the critical 3S in the lower level of *6-OST-1*, it suggests that *6-OST-1* and *3-OST-1* might not be physically coupled in a processive mode in making HS^{act} during biosynthesis.

It has been observed that two different sulfated domains are present in HS, the NS domain, and NAc/NS domains (40, 41). The NS domains consist of contiguous iduronosyl *N*-sulfoglucosamine units, whereas the NAc/NS domain consists of alternating *N*-acetylated and *N*-sulfated disaccharides. From the acceptor specificities of *6-OST-1*, *6-OST-2*, and *6-OST-3* using *N*-sulfated heparosan and desulfated re-*N*-sulfated heparin as substrate, it has been suggested that sulfation of position 6 of the *N*-sulfoglucosamine residues in the NS domain may be catalyzed by *6-OST-1*, whereas sulfation of position 6 of the *N*-sulfoglucosamine residues in the NA/NS domain may be catalyzed by 6-OST-2 and 6-OST-3 (2). Because there is no *6-OST-2* and *6-OST-3* in CHO cells, our results indicate that *6-OST-1* makes all 6-*O*-sulfated residues in CHO cells (Tables I and IV, Figs. 5 and 6). Furthermore, 30% reduction in *6-OST-1* activities in the mutant results in 3.7-fold reduction in HS^{act} production, which suggests that *in vivo* 6-*O*-sulfation of GlcNAc residues might be very sensitive to the level of *6-OST-1* activity. Indeed, overexpression of *6-OST-1* in the mutant results in the greatest increase in GlcNAc6S-containing disaccharide (Fig. 5). *In vitro* 6-*O*-sulfation at different time intervals (Fig. 6) also demonstrated that IdoUA2S-GlcNS is the preferred substrate for 6-*O*-sulfation. The *in vitro* studies (Fig. 6) may explain why GlcNAc6S-containing disaccharides were not observed in previous publications (2, 32, 42).

The mutant characterized in this manuscript is defective in AT binding (Fig. 2*E*), because it has decreased 6-*O*-sulfotransferase activities (Table II) and makes decreased amounts of 6-*O*-sulfated residues (Table I). The defect in this mutant can be corrected by both *in vivo* and *in vitro* 6-*O*-sulfations (Tables III and IV, Figs. 5–7). All the results show that 6-*O*-sulfotransferase-1 represents a critical enzyme in the anticoagulant HS biosynthetic pathway in CHO cells. However, the cause of decreased 6-*O*-sulfotransferase activities in the mutant is unclear. Because *6-OST-1* enzyme functions *in vitro*, a defect effecting an auxiliary protein is unlikely. The possibility remains that a defect in either mRNA stabilization or transla-

[2] L. Zhang, D. L. Beeler, and R. D. Rosenberg, unpublished observation.

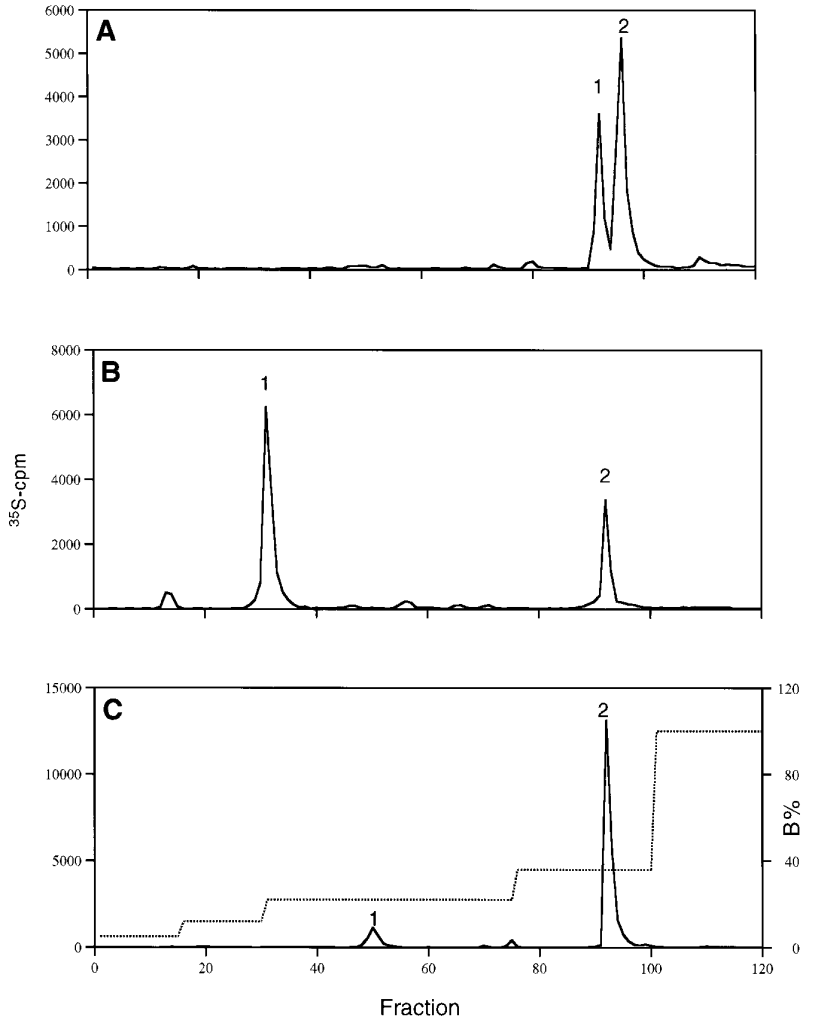

FIG. 8. **IPRP-HPLC of 6-*O*-sulfate-tagged HS^{act} di- and tetrasaccharides.** *In vitro* 6-*O*-sulfated and AT affinity-purified [^{3}H]HS^{act} oligosaccharides were digested with a mixture of heparitinases. The resulting di- and tetrasaccharides were separated on a Bio-Gel P6 column (see Fig. 7*C*). *A*, tetrasaccharides collected from Fig. 7*C*, *peak 1*: ΔUA-GlcNAc6^{35}S-GlcUA-GlcNS3S, *peak 2*: ΔUA-GlcNAc6^{35}S-GlcUA-GlcNS3S6^{35}S; *B*, disaccharides of the digested tetrasaccharides in the presence of HIP peptide; *peak 1*: ΔUA-GlcNAc6^{35}S, *peak 2*: ΔUA-GlcNS3S6^{35}S. *C*, disaccharides collected from Fig. 7*C*, *peak 1*: ΔUA-GlcNS6^{35}S, *peak 2*: ΔUA2S-GlcNS6^{35}S. The *broken line* indicates the gradient of acetonitrile.

TABLE IV
Disaccharide compositions of 6-O-sulfate-tagged HS^{act} oligosaccharides

In vitro 6-*O*-sulfated and AT-affinity purified [^{3}H]HS^{act} oligosaccharides were digested with a mixture of heparitinases. The resulting di- and tetrasaccharides were separated on a Bio-Gel P6 column (Fig. 7*C*). The tetrasaccharides collected from Fig. 7*C* were further degraded into disaccharides in the presence of HIP peptide. The disaccharides collected (Fig. 7*C*), and the disaccharides derived from the tetrasaccharides (Fig. 7*C*) were resolved by IPRP-HPLC with appropriate internal standards (Fig. 8) and quantitated. In duplicate experiments, the values varied by ≤15% of those shown.

Name	Percentage of total
	%
ΔUA-GlcNS**6**^{35}**S**	6
ΔUA2S-GlcNS**6**^{35}**S**	50
ΔUA-GlcNAc**6**^{35}**S**	29
ΔUA-GlcNS3S**6**^{35}**S**	15

tional competence is responsible for these effects. Unfortunately no good antibodies exist that would allow us to monitor the expression and the post-modification of *6-OST-1*.

6-*O*-Sulfation has been shown to be critical not only in AT binding, but also in FGF-FGFR interactions and other biologically important protein-HS interactions (5–11). The contributions of each *6-OST* isoform in generating specific biologically active HS sequences are unknown. Because *6-OST-2* and *6-OST-3* are not present in CHO cells, CHO wild-type cells and our *6-OST-1*-defective mutant cells are ideal for studying the *in vivo* and *in vitro* substrate specificity for *6-OST-2* and *6-OST-3* in terms of AT-binding, FGF-FGFR-activating, and other biologically relevant sequence generations.

Acknowledgments—We thank G. Paradis and M. Jennings in the Massachusetts of Technology FACS facility for assistance with flow cytometry. We thank J. D. Esko for providing 6-*O*-desulfated heparin and his insightful suggestions. We thank Dr. I. H. Segel for providing adenosine 5′-phosphosulfate kinase for making PAPS. We thank J. Zaia and C. E. Costello for their comments on the mass spectrometry data.

REFERENCES

1. Aikawa, J., Grobe, K., Tsujimoto, M., and Esko, J. D. (2000) *J. Biol. Chem.* **276,** 5876–5882
2. Habuchi, H., Tanaka, M., Habuchi, O., Yoshida, K., Suzuki, H., Ban, K., and Kimata, K. (2000) *J. Biol. Chem.* **275,** 2859–2868
3. Shworak, N. W., Liu, J., Petros, L. M., Zhang, L., Kobayashi, M., Copeland, N. G., Jenkins, N. A., and Rosenberg, R. D. (1999) *J. Biol. Chem.* **274,** 5170–5184
4. Bernfield, M., Gotte, M., Park, P. W., Reizes, O., Fitzgerald, M. L., Lincecum, J., and Zako, M. (1999) *Annu. Rev. Biochem.* **68,** 729–777
5. Lander, A. D., and Selleck, S. B. (2000) *J. Cell Biol.* **148,** 227–232
6. Lindahl, U. (1999) *Haemostasis* **29, Suppl. S1,** 38–47
7. Perrimon, N., and Bernfield, M. (2000) *Nature* **404,** 725–728
8. Rosenberg, R. D., Shworak, N. W., Liu, J., Schwartz, J. J., and Zhang, L. (1997) *J. Clin. Invest.* **100,** S67–S75
9. Rostand, K. S., and Esko, J. D. (1997) *Infect. Immun.* **65,** 1–8
10. Selleck, S. B. (2000) *Trends Genet.* **16,** 206–212
11. Shukla, D., Liu, J., Blaiklock, P., Shworak, N. W., Bai, X., Esko, J. D., Cohen, G. H., Eisenberg, R. J., Rosenberg, R. D., and Spear, P. G. (1999) *Cell* **99,** 13–22
12. Atha, D. H., Stephens, A. W., and Rosenberg, R. D. (1984) *Proc. Natl. Acad.*

Sci. U. S. A. **81,** 1030–1034
13. Atha, D. H., Lormeau, J. C., Petitou, M., Rosenberg, R. D., and Choay, J. (1985) *Biochemistry* **24,** 6723–6729
14. Atha, D. H., Lormeau, J. C., Petitou, M., Rosenberg, R. D., and Choay, J. (1987) *Biochemistry* **26,** 6454–6461
15. Lindahl, U., Backstrom, G., and Thunberg, L. (1983) *J. Biol. Chem.* **258,** 9826–9830
16. Lindahl, U., Thunberg, L., Backstrom, G., Riesenfeld, J., Nordling, K., and Bjork, I. (1984) *J. Biol. Chem.* **259,** 12368–12376
17. Shworak, N. W., Liu, J., Fritze, L. M., Schwartz, J. J., Zhang, L., Logeart, D., and Rosenberg, R. D. (1997) *J. Biol. Chem.* **272,** 28008–28019
18. Liu, J., Shworak, N. W., Fritze, L. M. S., Edelberg, J. M., and Rosenberg, R. D. (1996) *J. Biol. Chem.* **271,** 27072–27082
19. Zhang, L., Schwartz, J. J., Miller, J., Liu, J., Fritze, L. M., Shworak, N. W., and Rosenberg, R. D. (1998) *J. Biol. Chem.* **273,** 27998–28003
20. Zhang, L., Yoshida, K., Liu, J., and Rosenberg, R. D. (1999) *J. Biol. Chem.* **274,** 5681–5691
21. Loganathan, D., Wang, H. M., Mallis, L. M., and Linhardt, R. J. (1990) *Biochemistry* **29,** 4362–4368
22. Conrad, H. E. (1998) *Heparin-Binding Proteins*, Academic Press, San Diego, CA
23. Esko, J. D., Weinke, J. L., Taylor, W. H., Ekborg, G., Rodén, L., Anantharamaiah, G., and Gawish, A. (1987) *J. Biol. Chem.* **262,** 12189–12195
24. Esko, J. D., Stewart, T. E., and Taylor, W. H. (1985) *Proc. Natl. Acad. Sci. U. S. A.* **82,** 3197–3201
25. Esko, J. D., Elgavish, A., Prasthofer, T., Taylor, W. H., and Weinke, J. L. (1986) *J. Biol. Chem.* **261,** 15725–15733
26. Bai, X., and Esko, J. D. (1996) *J. Biol. Chem.* **271,** 17711–17717
27. Bai, X., Wei, G., Sinha, A., and Esko, J. D. (1999) *J. Biol. Chem.* **274,** 13017–13024
28. Wei, G., Bai, X., Gabb, M. M., Bame, K. J., Koshy, T. I., Spear, P. G., and Esko, J. D. (2000) *J. Biol. Chem.* **275,** 27733–27740
29. Zhang, L., Lawrence, R., Schwartz, J. J., Bai, X., Wei, G., Esko, J. D., and Rosenberg, R. D. (2001) *J. Biol. Chem.* **276,** 28806–28813
30. Dulbecco, R., and Vogt, M. (1954) *J. Exp. Med.* **99,** 167–182
31. Esko, J. D. (1989) *Methods Cell Biol.* **32,** 387–422
32. Habuchi, H., Kobayashi, M., and Kimata, K. (1998) *J. Biol. Chem.* **273,** 9208–9213
33. Yamada, S., Yoshida, K., Sugiura, M., Sugahara, K., Khoo, K. H., Morris, H. R., and Dell, A. (1993) *J. Biol. Chem.* **268,** 4780–4787
34. Yamada, S., Murakami, T., Tsuda, H., Yoshida, K., and Sugahara, K. (1995) *J. Biol. Chem.* **270,** 8696–8705
35. Shively, J. E., and Conrad, H. E. (1976) *Biochemistry* **15,** 3932–3942
36. Liu, J., Shriver, Z., Blaiklock, P., Yoshida, K., Sasisekharan, R., and Rosenberg, R. D. (1999) *J. Biol. Chem.* **274,** 38155–38162
37. Liu, S., Zhou, F., Hook, M., and Carson, D. D. (1997) *Proc. Natl. Acad. Sci. U. S. A.* **94,** 1739–1744
38. MacRae, I. J., Rose, A. B., and Segel, I. H. (1998) *J. Biol. Chem.* **273,** 28583–28589
39. Zaia, J., and Costello, C. E. (2001) *Anal. Chem.* **73,** 233–239
40. Jayson, G. C., Lyon, M., Paraskeva, C., Turnbull, J. E., Deakin, J. A., and Gallagher, J. T. (1998) *J. Biol. Chem.* **273,** 51–57
41. Lindahl, U., Kusche-Gullberg, M., and Kjellen, L. (1998) *J. Biol. Chem.* **273,** 24979–24982
42. Habuchi, H., Habuchi, O., and Kimata, K. (1995) *J. Biol. Chem.* **270,** 4172–4179